Mining, Metallurgy & Exploration (2022) 39:793–804
https://doi.org/10.1007/s42461-021-00489-6

Comparison of the Antimony Cementation from Chloride Media Using Various Cementators

Özgün Küçükoğlu[1,2] · Burcu Nilgün Çetiner[2] · Mehmet Hakan Morcalı[3] · Serdar Aktaş[2]

Received: 22 December 2020 / Accepted: 10 September 2021 / Published online: 28 January 2022

Abstract
This study compares the cementation performance of metallic iron, metallic aluminum, and metallic tin in terms of the reaction conditions and parameters in synthetic antimony chloride solutions. The effects on the antimony recovery (%) caused by the cementators' types, stirring speed, reaction time, and temperatures were explored thoroughly. The cementation kinetics of antimony were also explored for each cementator. The activation energies were determined to be 10.99, 9.09, and 13.58 kJ mol^{-1} for Al, Fe, and Sn, respectively. The results reveal that the reaction is diffusion controlled, and comparable results were obtained for each cementator. At 25 °C, 40 mg of iron powder was found to reduce all antimony ions (i.e., approx. 99% recovery), but even when 100 mg of Al and Sn cementators were used, the antimony recovery did not reach 100%. This result shows that iron is the best candidate to cement antimony out of the solution.

Keywords Cementation · Reduction · Replacement · Antimony · Chloride media

1 Introduction

Antimony has been a metal of interest for different purposes since the Early Bronze Age, and recently, it has had a wide variety of uses as a flame retardant (70% of the market share), alloying element, catalyst, a component in brake linings, and medical substances (including for AIDS treatment). Its uses have also extended to the energy industry as a dopant in n-type silicon wafers. Thus, besides natural sources, antimony is contained in waste produced as a result of anthropogenic activities. The concentration of antimony in the earth's crust is in the range of 0.2 to 0.3 ppm, but every year, the antimony released due to anthropogenic activities is thousands of tons [1–2].

The consumption of rainwater contaminated by antimony sources rarely has toxic effects in developed countries [2]. There are restrictions on the use and handling of antimony defined by The American Conference of Governmental Industrial Hygienists and the Deutsche Forschungsgemeinschaft as a potential carcinogen, and the US Food and Drug Administration allow levels of only 2 ppm in food [2]. Antimony mining and smelting sites are some of the most environmentally polluted areas due to high levels of antimony accumulation and very low bioavailability (particularly metabolization of antimony ions by plants—i.e., fixation of antimony in the soil). Even 100 years after the closure of mining or smelting activities, the soils remain unchanged unless the antimony residuals oxidize [3].

In aqueous systems, antimony ions are found in both (+3) and (+5) oxidation forms as antimonic acid, antimonious acid, antimonite, antimonate, and sulfidic complexes [4]. Predominantly, the pentavalent oxyanion of antimony is more dominant in soils. Inorganic antimony species are more harmful than organic ones, and the trivalent form is more toxic than the pentavalent form [5–9]. There are two main approaches to avoid environmental risks associated with antimony pollution:

✉ Serdar Aktaş
serdaraktash@yahoo.com

Özgün Küçükoğlu
ozgunkucukoglu@gmail.com

Burcu Nilgün Çetiner
burcunilguncetiner@gmail.com

Mehmet Hakan Morcalı
hakanmorcali@gmail.com

[1] Vocational School, Mechanics Department, Beykent University, Esenyurt/İstanbul,, Turkey

[2] Department of Metallurgical and Materials Engineering, Marmara University, 34722 Istanbul, Turkey

[3] Naci Topcuoglu Vocational High School, Gaziantep University, 27600 Gaziantep, Turkey

(i) Understanding the transport and redox mechanism of antimony species and their behavior in the environment
(ii) Preventing the release of antimony ions into the ecosystem by developing more straightforward methods to manage antimony-containing wastes.

For the first method, the latest studies show that most of Sb(III) is oxidized into Sb(V) on the surface of soils under aerobic conditions. In contrast, only a minority of Sb(III) is oxidized under anaerobic conditions; therefore, the leakage of trivalent antimony ions is possible in anoxic conditions in acidic soils, and water contamination by the more dangerous Sb (III) may occur. Continuous pollution with pentavalent antimony ions after oxidation of the trivalent antimony ions occurs in calcareous soils [10], as has occurred in abandoned antimony mines in the Western Carpathians, Slovakia [11].

There are various techniques for the extraction and/or recovery of antimony ions from aqueous media and soils, such as:

(i) Selective leaching of antimony using 0.4 M KOH, NaOH, and Na_2S, sodium sulfide leaching, pressure oxidation, concentration, and crystallization steps to obtain sodium pyroantimonate and alkaline xylitol solution as extraction agents [12–17]
(ii) Electrodeposition, electrorefining, electrowinning, or electrocoagulation using aluminum electrodes in flotation wastewater from antimony mines [17–21]
(iii) Reductive leaching using nitrogen gas purging followed by hydrochloric acid, hydrochloric acidified potassium dichromate solution, and cyanidation leaching [22]
(iv) Ozonation leaching by hydrochloric acid and ozone purging, which can also be used as a pretreatment [23–25]
(v) Membrane electrowinning following a chlorination–oxidation procedure of stibnite concentrate or hydrolysis after chlorination–oxidation of stibnite concentrate and then sulfide precipitation by ammonium sulfide, after which hydrolysis neutralization and crystal transformation by ammonia and ethylenediaminetetraacetic acid tetrasodium salt (EDTA) [26] can be applied.

These techniques provide economic benefits apart from environmental concerns. For example, an average ton of waste mobile phones contains 1 kg of antimony and other metallic substances of value. Thus, instead of mining activities, the recovery of antimony from electronic waste is much more beneficial. For example, it is estimated that 1023 tons of antimony-containing mobile phone waste will be generated in China in 14 years [27]. This amount of antimony can be recovered using these techniques. Nevertheless, although these methods seem advantageous compared to other recycling techniques, they require significant investment costs. Furthermore, none of these methods involve antimony production.

It is cheaper and more practical to obtain antimony in a fine form using the cementation method, which requires no pre-investment cost in applying the method. Furthermore, it can be easily adapted to industry, which is one of the most important advantages.

Trials were conducted to check if the cementation process occurs because the solution's acidity is too low in some cases, and the type of the acid also matters. In a study by Aktas et al. [28], rhodium failed to precipitate from a sulfate solution with the addition of copper powder; therefore, rhodium sulfate was first precipitated as rhodium hydroxide ($Rh(OH)_3$) and then converted to rhodium chloride in HCl solution. However, rhodium is a more noble metal than copper and is expected to be cemented in a sulfate-containing medium, but this cementation reaction would not occur due to kinetic factors [29].

Similar observations were also made in another study by Aktas et. [30], where silver cementation (%) increased with increasing quantities of zinc. A series of experiments were designed and performed to analyze the cementation behavior of antimony ions in an acidic medium and to optimize the cementation conditions at the laboratory scale. The results were evaluated in the context of various factors such as time, temperature, stirring rate, pH, and the amount of the cementator in this study.

The cementation method involves reducing metal ions in a solution to a metallic state by an electrochemically more negative metal in the solution, such as metallic zinc or aluminum, among others [31–36]. The standard oxidation/reduction potentials of Al, Fe, Sn, and Sb are presented in Table 1.

The potential difference is calculated as 1.884 V for aluminum cementation, 0.648 V for iron cementation, and 0.348 V for tin cementation [37]. Thus, aluminum, iron, and tin have the potential to cement antimony out of solution. Therefore, antimony ions are reduced by the cathodic reaction.

The cell potentials of reactions are calculated by E^0 (reduction) – E^0 (oxidation):

Table 1 The standard reduction potentials of Al, Fe, Sn, and Sb [37]

Redox half-reaction	Potential vs. standard hydrogen electrode (SHE), E°(V)
$Al^{3+} + 3e^- \rightarrow Al°$	– 1.676
$Fe^{2+} + 2e^- \rightarrow Fe°$	– 0.44
$Sn^{2+} + 2e^- \rightarrow Sn°$	– 0.14
$SbO^+ + 2H^+ + 3e^- \rightarrow Sb° + H_2O$	+ 0.208

$$\begin{aligned} &SbO^{+}\,(aq) + 2H^{+}\,(aq) \\ &+Al^{\circ}(s) \rightarrow Sb^{\circ}(s) + Al^{3+}\,(aq) \\ &+H_2O \quad E^0 = 1.874\ V(n = 3) \end{aligned} \tag{1}$$

$$\begin{aligned} &SbO^{+}\,(aq) + 2H^{+}\,(aq) \\ &+3/2Fe^{\circ}(s) \rightarrow Sb^{\circ}(s) \\ &+3/2Fe^{2+}(aq) + H_2O \quad E^0 = 0.659\ V(n = 3) \end{aligned} \tag{2}$$

$$\begin{aligned} &SbO^{+}\,(aq) + 2H^{+}\,(aq) \\ &+3/2Sn^{\circ}(s) \rightarrow Sb^{\circ}(s) \\ &+3/2Sn^{2+}(aq) + H_2O \quad E^0 = 0.35\ V(n = 3) \end{aligned} \tag{3}$$

Thus,

$$\Delta G^{o} = -nFE^{o} \tag{4}$$

According to Eq. 4, the standard free energy change of all reactions is negative (−542.44 kJ mol^{-1} for Eq. 1, −190.75 kJ mol^{-1} for Eq. 2, and −101.31 kJ mol^{-1} for Eq. 3). The variable n is the number of transferred electrons, and F is the Faraday constant (96,485 C mol^{-1} e^{-}). This means that all reactions are spontaneous in their standard conditions.

At the end of the cementation process, the remaining Sb concentration of the solution can be calculated by the Nernst equation:

$$E = E^{o} - (RT/nF)\ lnQ \tag{5}$$

From these values, it can be recognized that the cementation reactions of antimony given in Eqs. 1–3 proceed to the right, and the reverse reaction is almost out of the question [38]. More information was provided in the supplementary file. It is expected that if a metal (antimony in this case) has a higher reduction potential than its cementator, it can be thermodynamically reduced by the addition of the cementator in a solution containing these metal ions. Owing to the difference between the standard electrode potentials of antimony and the cementator, the cementator anodically dissolves, and Sb^{3+} ions become neutral and precipitate. The low ratio of concentrations indicates an exceptionally low concentration of antimony ions remaining in the solution. As a result, antimony can be effectively recovered by cementing with aluminum, iron, or tin [39].

In addition to these reactions, there are also three reactions that may occur during the cementation process. These reactions are reduction of antimony with Fe^{2+}, H_2, and Sn^{2+} given in equations, respectively:

$$Sb^{3+} + 3Fe^{2+} \rightarrow Sb^{o} + 3Fe^{3+} \quad E = -0.559\ V \tag{6}$$

$$2Sb^{3+} + 3H_2 \rightarrow 2Sb^{o} + 6H^{+} \quad E = 0.208\ V \tag{7}$$

$$2Sb^{3+} + 3Sn^{2+} \rightarrow 2Sb^{o} + 3Sn^{4+} \quad E = 0.061\ V \tag{8}$$

The reduction of antimony with Fe^{2+} ions (e.g., Eq.6) is not a spontaneous reaction due to its positive ΔG value. On the other hand, antimony can be reduced by hydrogen molecules (i.e., Eq. 7) generated by the dissolution of the cementator. However, as long as the hydrogen molecules are formed by the dissolution of the cementator, there is no significant difference between hydrogen and cementator reduction (in net reaction, the hydrogens cancel each other). Apart from all this, Eq. 8 indicates that Sn^{2+} should make a significant contribution to the antimony cementation. The precipitation efficiency of antimony increases when tin reaches its maximum oxidation state. Therefore, we can rewrite the antimony cementation equation for tin as:

$$\begin{aligned} &SbO^{+}(aq) + 2H^{+}(aq) \\ &+3/4Sn^{\circ}(s) \rightarrow \quad Sb^{\circ}(s) \\ &+3/4Sn^{4+}(aq) + H_2O \quad E_0 = 0.201\ V \\ &\qquad\qquad\qquad\qquad (n = 3) \end{aligned} \tag{9}$$

Considering all of this, 1 g Sb could be reduced by 0.22 g Al, 0.69 g Fe, and 0.73 g Sn. In this study, all the data were given as "mg" because it is preferred in industrial applications. Nevertheless, the equivalent molar amount and the stoichiometric ratios of cementators are given in Table 2.

Studies related to antimony cementation are very scarce, even though they may contribute to pyrometallurgical processes that could be widely used for antimony extraction. Hence, in this study, the aim was to determine the reduction conditions for antimony ions in solution. Metallic aluminum, iron, and tin powders were used as cementators, and the effects of experimental parameters were investigated in depth.

2 Experimental Procedure

Antimony(III) chloride (≥99%, Sigma Aldrich) was selected as the initial antimony compound. The initial antimony solution was prepared with 1000 ppm of antimony by adding 0.1% (*w*/w) L-tartaric acid (Merck) and 10% (*v*/v) hydrochloric acid solution to obtain a stable antimony complex, thus preventing its precipitation unexpectedly. All of the chemicals used in this study were of analytical purity. Optimum cementation parameters were determined by examining factors such as the time, temperature, and amount of cementators (i.e., aluminum, iron, and tin). A TSB-28C shaking water bath was used in the experiments. After each cementation experiment, solid/liquid separation was performed using filter paper.

Table 2 Equivalent molar amount of cementators

	Al		Fe		Sn	
mg	mmole	S.R.*	mmole	S.R.*	mmole	S.R.*
10	0.37	2.26	0.18	0.73	0.08	0.68
20	0.74	4.51	0.36	1.45	0.17	1.37
30	1.11	6.77	0.54	2.18	0.25	2.05
40	1.48	9.03	0.72	2.91	0.34	2.74
50	1.85	11.28	0.90	3.63	0.42	3.42
60	2.22	13.54	1.10	4.36	0.51	4.10
70	2.59	15.79	1.25	5.09	0.59	4.79
80	2.96	18.05	1.43	5.81	0.67	5.47
90	3.34	20.31	1.61	6.54	0.76	6.15
100	3.71	22.56	1.79	7.27	0.84	6.84

* Stoichiometric ratios of Al, Fe, and Sn with respect to Eqs. 1, 2, and 9

The concentration of antimony in the solutions was determined by using an Atomic Absorption Spectrophotometer (AAS, Shimadzu AA-7000, Japan). While operating the instrument, the recommended standard conditions were used. A standard stainless steel nebulizer and the standard acetylene burner head were used. The operating parameters for the AAS were as follows: wavelength, 217.6 nm; slit width, 0.5 nm; fuel gas flow, 2.0 L/min; lighting mode, BGC-D_2; and type of oxidant, air. All measurements were carried out using the recommended cookbook of the Shimadzu cooperation for analyzing antimony. The X-ray diffraction (XRD) analysis of the cemented antimony was carried out in the 2θ range of 5–105° using a Rigaku vertical diffractometer with Cu-Kα radiation, a step size of 0.02° (2θ), 2 s intervals, 40 mA, and 40 kV. The recorded phases that generated the diffraction pattern were identified using JADE 6.0 (Rigaku).

Before starting the XRD analysis of the cemented antimony powder, it was treated with 0.1 M HCl (pH ~ 1), distilled water, and then acetone to remove the possible cementator residue. This washing process was performed to remove any possible cementator residue. The powders were then dried under a vacuum at 80 °C for 1 h. The fine powder was subsequently placed in the holder of the instrument. The specimen was also used for scanning electron microscopy-energy dispersive spectroscopy (SEM-EDS) analysis with ZEISS EVO LS10, Japan.

Table 3 shows the specific amount of cementator used in each experiment to reduce the antimony in the solution. For each experiment, 20 mL of stock antimony solution with the addition of cementator was transferred to 50-mL centrifuge tubes. An experimental study was carried out in a temperature-controlled water bath to obtain a uniform temperature distribution and heat convection. The experimental conditions are given in Table 3. The recovery efficiency (%) of this cementation process was calculated using the following equation:

Table 3 Experimental conditions

Parameters	Type of cementators	Ranges
	Aluminum	10–100 mg
	Iron	10–100 mg
	Tin	10–100 mg
Stirring speed		100–600 rpm
Temperature		25–55 °C
Time		15–180 min

$$Recovery(\%) = \left[\frac{(C_0 - C_t)}{C_0}\right] \times 100 \quad (10)$$

where C_0 is the initial antimony concentration and C_t is the final antimony concentration at the end of the experiment. The results of each sample were compared graphically after measurements.

3 Results and Discussion

3.1 Effect of Cementator Type

The effect of the cementator type and the quantity on the recovery of antimony was investigated. The experiments were carried out using 20 mL of Sb^{+3} at 1000 ppm with stirring at 200 rpm for 60 min and 25 °C. Figure 1 shows the recovery (%) of antimony as a function of the cementator type and quantity. As shown in the figure, all three metal powders can ensure that antimony can be recovered.

Depending on the cementator type and the quantity, the amount of antimony recovery varied. For example, 40 mg of iron powder was found to be enough for nearly 100% recovery, but in the case of tin, the amount increased to 100 mg, and for aluminum, the antimony recovery did not attain

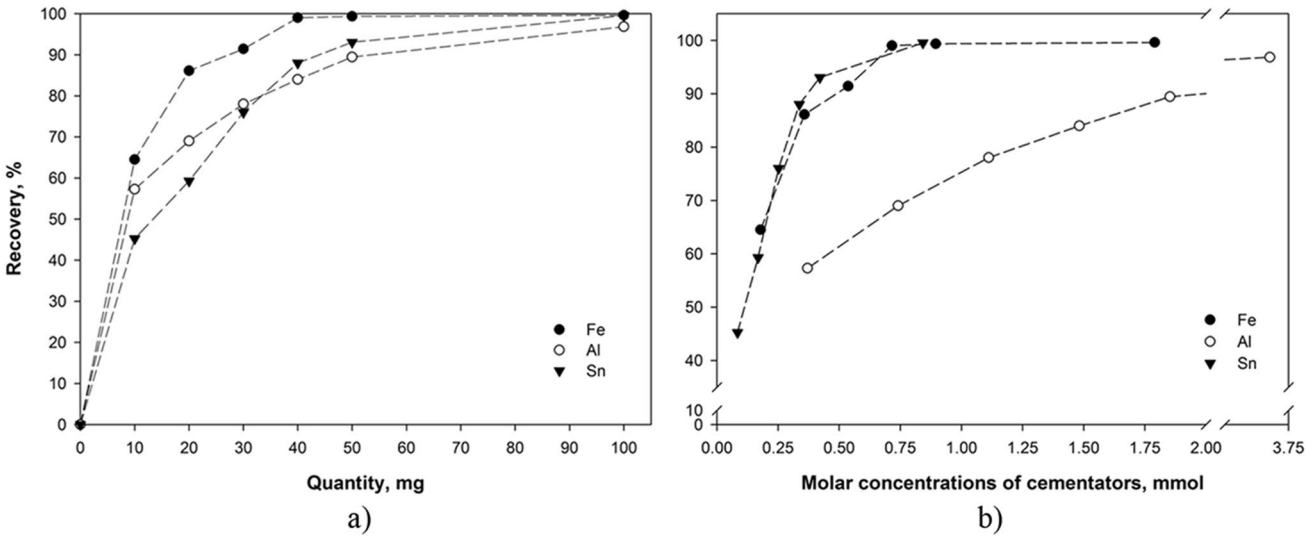

Fig. 1 Recovery of antimony as a function of cementator type and (a) Quantity (mg), (b) Molar concentrations of cementators (mmol) (20 mL of Sb^{+3} at 1000 ppm, 200 rpm, 60 min, 25 °C)

100% even if 100 mg was used. By increasing the amount of active metal, iron, tin, and aluminum per antimony ion, the surface area at interaction was increased, and a higher rate of metallic antimony recovery was achieved [28–30]. Similar cementation studies showed that increasing the amount of zinc as the active metal increases the yield percentage of silver cementation [30].

On the other hand, as seen in Fig. 1a, antimony recovery in tin cementation reached 45%, which is an expected phenomenon even when only 10 mg Sn has been employed. This result proves that a certain amount of antimony was reduced by Sn(II), as given in Eq.8.

Assuming that all the cementators have been dissolved in solution, we can obtain the molar concentrations of cementators, as seen in Fig. 1b. Figure 1b clearly shows that the behavior of Sn and Fe is almost identical for antimony reduction. The same amount of cementator (Fe and Sn) reduces the same amount of antimony, and it reaches the maximum value near 0.75 mol for each cementator. In other words, all antimony in solution (20 mg, 0.164 mmol) can be recovered using 0.75 mol of Fe and Sn. On the other hand, aluminum behaves differently with respect to the other cementators. It reaches the maximum value at 3.75 mol, which is five times more than the other cementators. This phenomenon occurs because aluminum is preferentially dissolved by the free acid.

3.2 Effect of Stirring Speed

Experiments to investigate the effect of stirring rate were carried out using 20 mL of Sb^{+3} at 1000 ppm with 30 mg of the cementators (Al, Fe, or Sn) for 60 min at 25 °C. Although the maximum recovery for Sb was obtained at cementator amounts above 40 mg in the previous experimental series, 30 mg of cementators have been chosen to highlight the effect of stirring speed. The antimony recovery (%) increased with the rate of stirring, which was helpful for the interaction of antimony ions with cementator metal particles and the acidic medium. There were two mechanisms: the cementation process and the reaction of the acidic medium with the active metal particles (iron, tin, and aluminum). The second reaction is an excessive consumption reaction. The use of stirring or shaking in this procedure increases the possibility of interaction of the active metal particles with the acidic medium, thus facilitating their dissolution and the transportation of dissolved solute (Fig. 2).

3.3 Effects of Temperature and Time

A series of experiments were performed to observe the effect of temperature and time using 20 mL of Sb^{+3} at 1000 ppm with 10 mg of cementators (Al, Fe, or Sn) for 180 min at 200 rpm and different temperatures (25 °C, 35 °C, 45 °C, and 55 °C). As shown in Figs. 3, 4, and 5, the temperature and time had important roles in the cementation, like in previous works [28–30]. The temperature promoted the reaction between the active metal particles and antimony ions. As the temperature increased from 25 °C to 55 °C, the antimony recovery increased. Within 60 min, the Sb recovery percentage increased from 53% to 69% when using Al, from 62% to 75% when using Fe, and from 41% to 61% when using Sn.

After 3 h of cementation at 25 °C, there was almost 67% Sb recovery in the case of Al, 71% Sb recovery in the case of Fe, and 61% Sb recovery in the case of Sn.

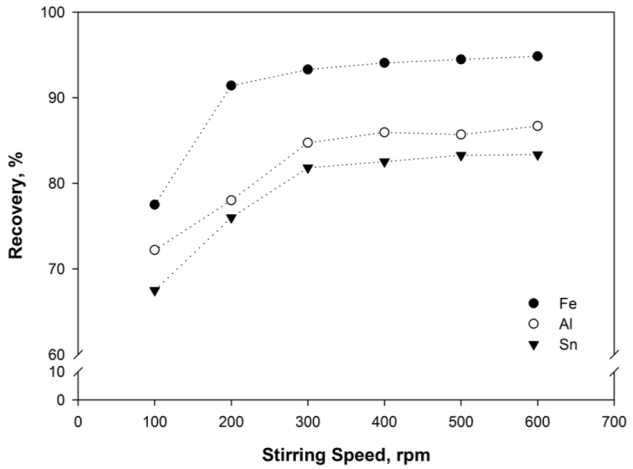

Fig. 2 Recovery of antimony as a function of cementator type and stirring speed (20 mL of Sb^{+3} at 1000 ppm, 30 mg of cementator, 60 min, 25 °C)

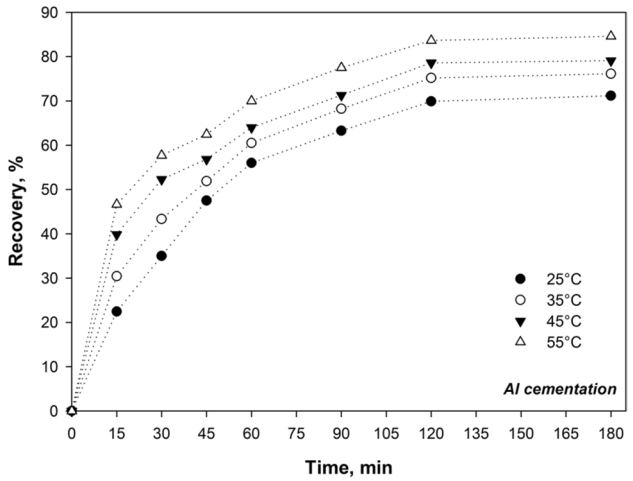

Fig. 3 Recovery of antimony as a function of temperature and time (20 mL of Sb^{+3} at 1000 ppm, 300 rpm, 10 mg of Al)

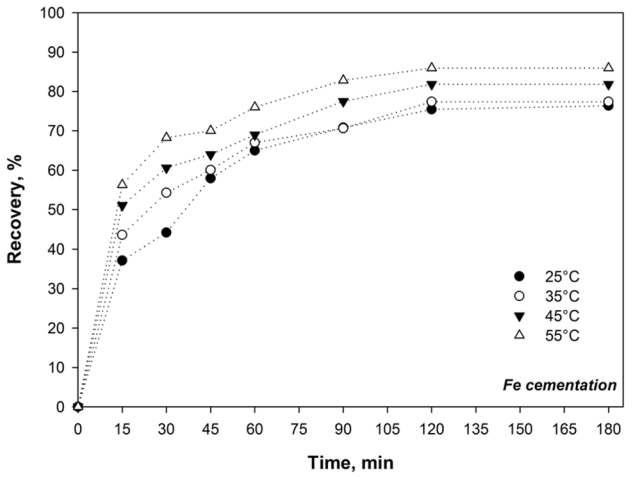

Fig. 4 Recovery of antimony as a function of temperature and time (20 mL of Sb^{+3} at 1000 ppm, 300 rpm, 10 mg of Fe)

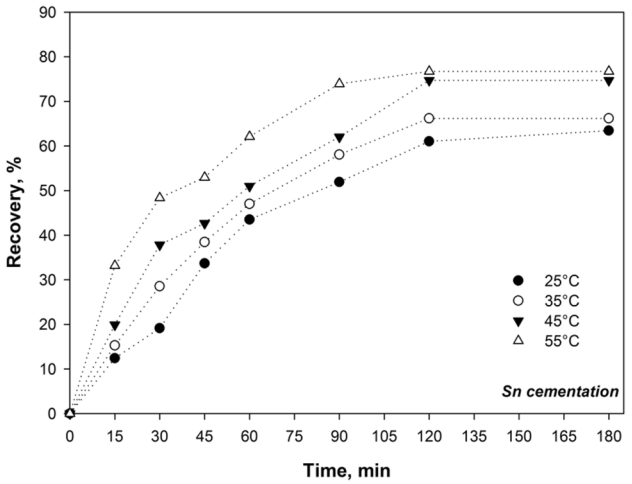

Fig. 5 Recovery of antimony as a function of temperature and time (20 mL Antimony^{+3}, 300 rpm, 10 mg of Sn)

However, at 55 °C, the Sb recovery efficiency increased noticeably from 67 to 80% with Al, 71 to 83% with Fe, 61 to 75% with Sn. Thus, it can be concluded that increasing the temperature has a significant effect on the antimony recovery by cementation, i.e., an increase of approximately 20% was obtained when the temperature was increased from 25 °C to 55 °C.

When we compare the cementation efficiencies concerning time, the antimony recovery slightly increased with increasing time after 45 min for Al and Fe, as seen in Figs. 4 and 5. On the other hand, as seen in Fig. 6, the increase in antimony recovery efficiency for Sn cementation increased rapidly after 45 min. This situation is the consequence of taking time to reach the 4+ oxidation state of tin.

3.4 Cementation Kinetics

The kinetic model can be calculated from the reaction order using experimental data with the integrated rate law. The cementation kinetics of the antimony cementation process values were extracted from Figs. 3, 4, and 5, and various kinetic models were investigated to uncover the underlying mechanism (e.g., one-dimensional diffusion, two-dimensional diffusion, three-dimensional diffusion, first-order, etc.). The studied kinetic models and their equations are given in Table 4.

Among all the computed kinetic equations, the two-dimensional diffusion for aluminum, the three-dimensional diffusion for iron, and the first-order kinetics for tin best fitted the antimony cementation results, as shown in Fig. 6. A

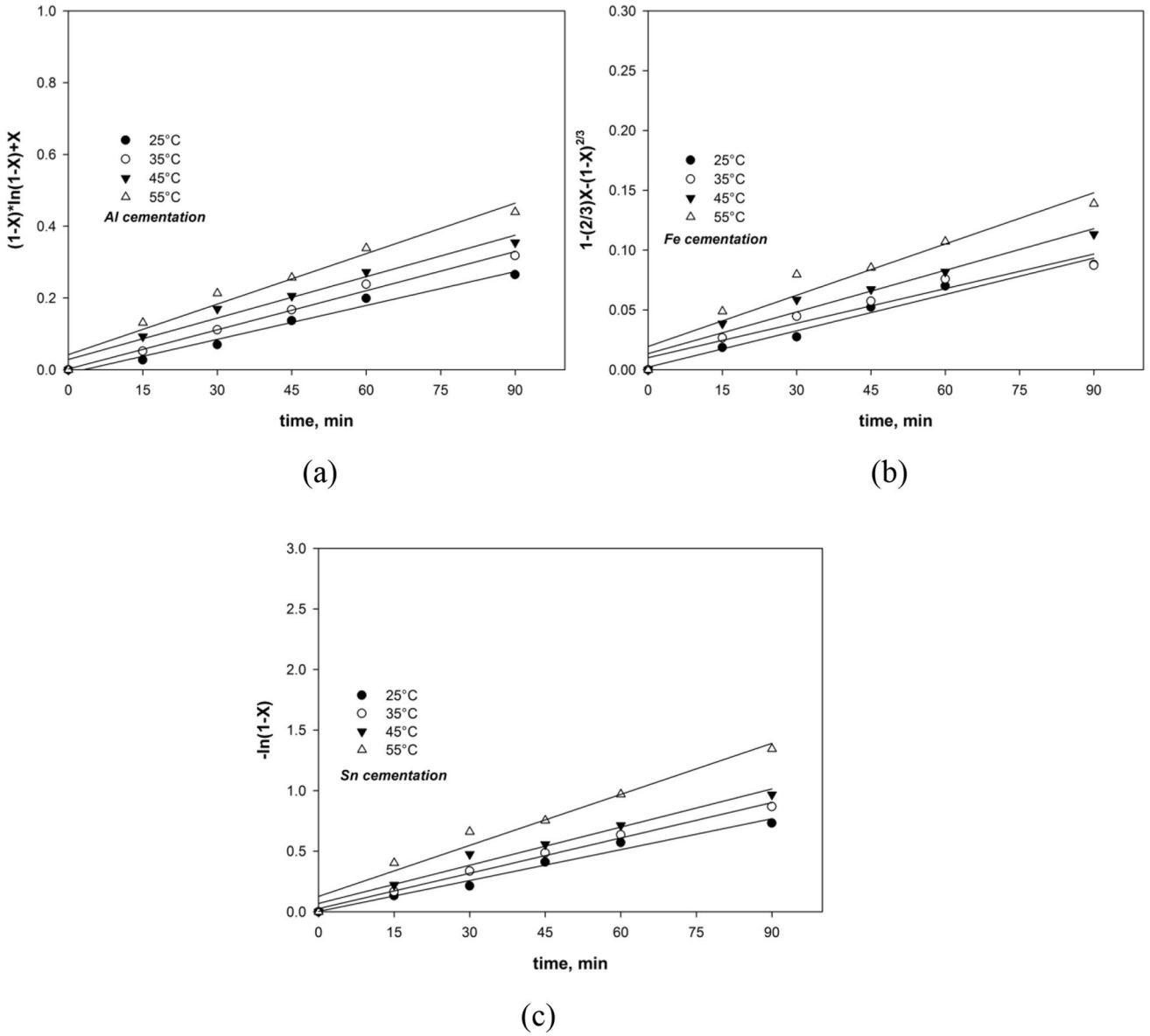

Fig. 6 Relationship between (a) [(1–X)*ln(1–X) + X)] for aluminum, (b) [1–(2/3X)–(1–X)$^{2/3}$] for iron, and (c) –ln(1–X) for tin and time as a function of temperature

Table 4 The studied kinetic models [40]

Reaction model	Kinetic equation
Two-dimensional diffusion	$(1–X)\ \ln(1–X)+X=kt$
Three-dimensional diffusion	$1–(2/3)X–(1–X)^{2/3}=kt$
Jander eq. (3D)	$[1–(1–X)^{1/3}]^2=kt$
First-order kinetics	$–\ln(1–X)=kt$
Two-dimensional phase boundary reaction	$1–(1–X)^{1/2}=kt$
Three-dimensional phase boundary reaction	$1–(1–X)^{1/3}=kt$
Avrami equation	$[-\ln(1 –X)]^{1/2}=\mathrm{kt}$
Erofeev equation	$[-\ln(1 –X)]^{1/3}=\mathrm{kt}$

k is the rate constant, t is the time (min), and X is the fraction of extracted antimony in the $SbCl_3$ solution

high coefficient of correlation was derived by fitting experimental data, which implied a diffusion-controlled process. Accordingly, Arrhenius plots were obtained using the equations extracted from Fig. 7.

The plots in Fig. 7 were obtained using the Arrhenius equation given in Eq. 11, and the activation energies (E_a) were calculated from the plotted figures.

$$\mathrm{In\ k} = \mathrm{lnA}\ E_a/R * 1/T \tag{11}$$

k is the rate constant, Ea is the activation energy (J mol^{-1}), R is the gas constant (8.314 J mol^{-1} K^{-1}), and T is the temperature in Kelvin (K). A is known as the frequency factor

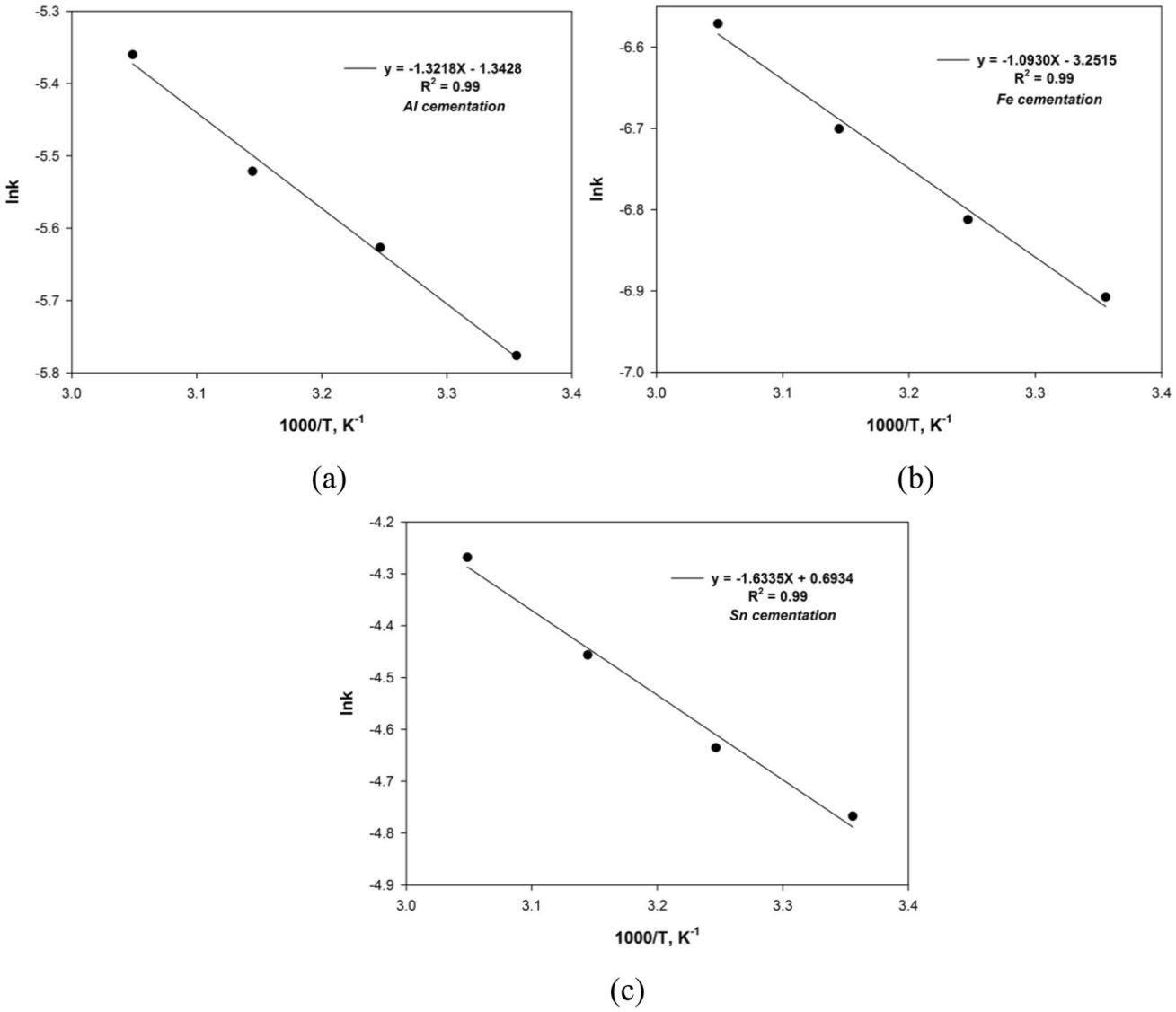

Fig. 7 Arrhenius plot using related kinetic models for (a) aluminum, (b) iron, and (c) tin

and has units of L mol^{-1} s^{-1}. It considers the frequency of reactions and the likelihood of correct molecular orientation. The activation energies of reactions can be calculated by multiplying the negative slope of the line with the gas constant R. Thus,

For Al cementation, Ea = 10.99 kJ/mol
For Fe cementation, Ea = 9.09 kJ/mol
For Sn cementation, Ea = 13.58 kJ/mol

3.5 Characterization of the Obtained Powders

Following the production of metallic antimony powder, the powder was treated with 0.1 M HCl (pH = ~1), distilled water, and then acetone. Next, the powders were dried under a vacuum at 80 °C for 1 h. Before XRD and SEM-EDS analysis, these agglomerated powders were ground to finer powder using an agate mortar. The antimony content was found to be 90.39% without the removal of impurities (i.e., before HCl treatment).

Figure 8b shows that all diffraction peaks belong to antimony powder, which is available as single-phase antimony after HCl treatment; however, there are some unreacted Fe and by-products of the cementation process, antimony oxychloride, which co-exist with antimony metal at the end of the cementation process before the HCl treatment, as shown in Fig. 8a.

This result is consistent with the EDS results shown in Fig. 9b and 10b of "spot 2". According to the SEM images

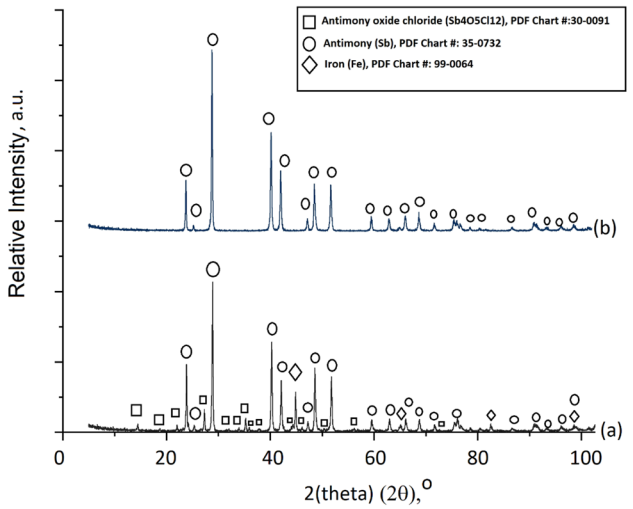

Fig. 8 Phase identification of the antimony metal obtained with the antimony cementation process using iron as a cementator (a) before HCl treatment and (b) after HCl treatment

shown in Figs. 9a and 10a, the porous structure consists of submicron particles of less than 1 µm, and the powder had a typical cemented powder structure. After the HCl treatment process, most of the impurities were successfully removed, and the powder of almost analytical purity was obtained.

In addition to that, comparison of Figs. 9 and 10 shows the precipitated cementators along with antimony. According to the figures, 9.61 wt% of iron precipitates without treatment with HCl. These precipitates can be easily removed by HCl treatment, which has almost no action on antimony. Removal of cementators by HCl treatment is also applicable to both Al and Sn.

4 Conclusions

The determination of cementation parameters is of paramount importance to the redox reactions. As demonstrated, the three competitive cementators were found to precipitate

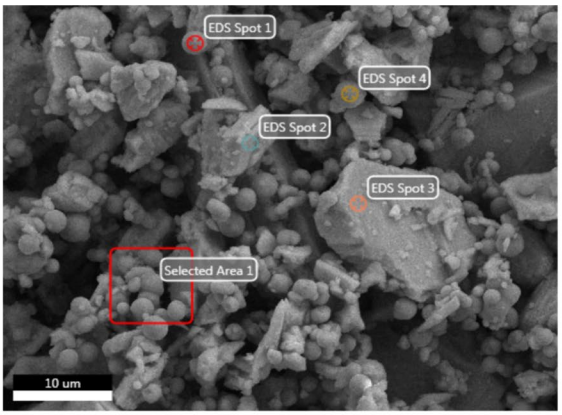

(a)

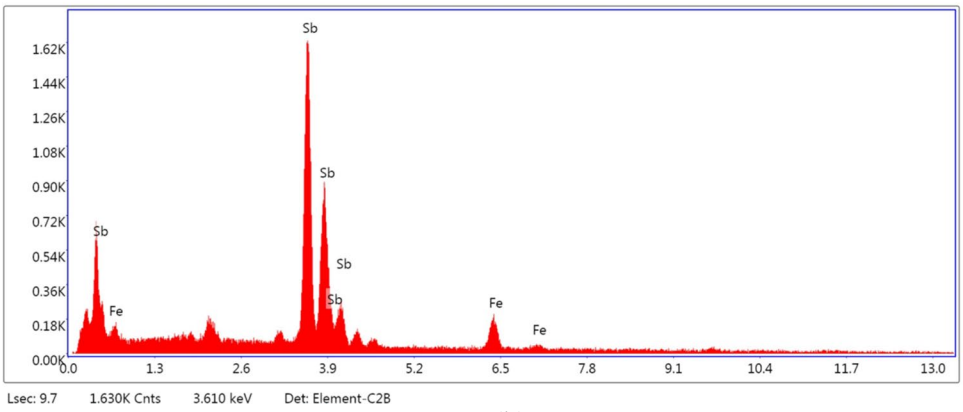

(b)

Fig. 9 SEM-EDS images of antimony powder before HCl treatment

Element	Weight %	Atomic %
Sb-L	90.39	81.18
Fe-K	9.61	18.82

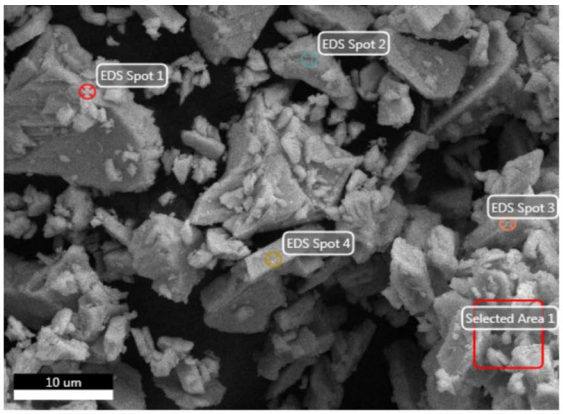

(a)

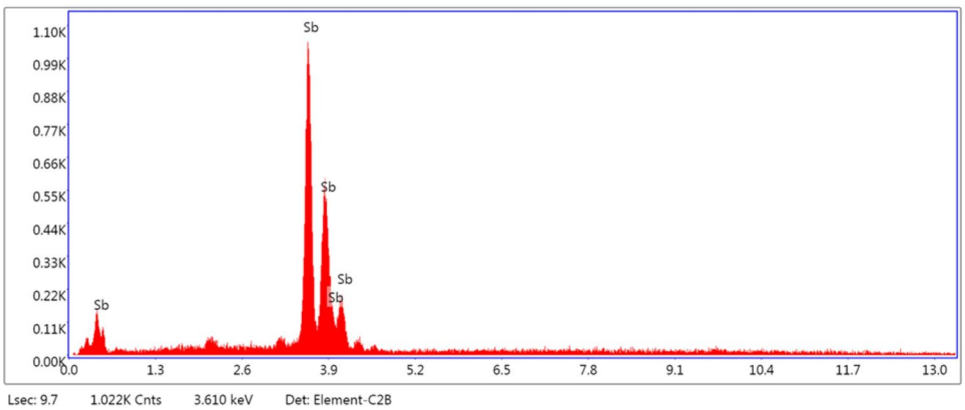

(b)

Element	Weight %	Atomic %
Sb-L	100.00	100.00

Fig. 10 SEM-EDS images of antimony powder after HCl treatment

the antimony out of the solution effectively. The main objectives of this work are to put forward an applicable and straightforward process to achieve high recovery efficiency of antimony under ambient atmospheric conditions. It is well known that the metal prices vary over time. For example, in the early 2010s, the price of antimony was twice the price of tin. In addition, antimony is one of the critical raw materials (CRM) according to the European Commission due to its lack of reserves. Thus, the price of antimony is expected to increase in the near future, which was our motivation to undertake this research work. For these reasons, the comparison of the price of the metals is beyond the scope of the current study.

Nevertheless, if one must compare today's cementator prices (August 2021), Scrap Fe is 466.5 US$, Al is 2618.5 US$, and Sn is 36,065 US$ per ton [41]. Considering that the current price of antimony is 6129 US$ per ton [42], Fe is the most cost-effective candidate as a cementator. On the other hand, because tin is more expensive than antimony, it is not economically viable to use tin in the cementation process. However, metal prices can change over time as mentioned before.

At 25 °C, 40 mg of iron powder was found to reduce almost all antimony ions (i.e., approx. 99% recovery), but even if 100 mg of aluminum and tin were used, the antimony recovery did not reach 100%. As the temperature increased from 25 °C to 55 °C, the antimony recovery was found to increase. With no extra heating, the Sb recovery percentage can be increased just by increasing the reaction time because the possibility of interactions is increased in both cases. These valuable results proved that there is a synergetic interaction between the reaction temperature and time.

The obtained activation energies indicated that the reactions are diffusion-controlled for each cementator, the use of the stoichiometric amount of cementators in the solution, where there is no interaction between the components, has little or no effect on the reducing behavior of the trivalent antimony ions. However, the situation changes dramatically when increasing the quantity of the cementators, which can interact with the trivalent antimony ions through

replacement, and the recovery percentage of antimony is increased significantly.

The cementation process plays a key role in not only producing metallic material but also in metallurgical and environmental science for the synthesis of new metallic material and cleaning, removing undesirable compounds from a solution, or replacing a hazardous element with a less hazardous element to protect the environment. Iron showed the best performance. When all the experimental results are examined, considering the economic factors, the best candidate for obtaining antimony from acidic antimony solutions is iron powder. It is well known that iron is the most inexpensive and second most abundant metal and iron shavings can be readily found everywhere. Further studies are necessary to fully understand how these factors interact, to use this knowledge to help design a new experimental setup, and to reduce the cementator consumption.

Symbols Co: Concentration of Sb in $SbCl_3$ solution; Ct: Concentration of Sb in solution after cementation for time t; t: Cementation time (min); F: Faraday constant; n: Number of electrons transferred in the oxidation-reduction reaction; E°: Standard potential of the chemical reaction; K_{eq}: Equilibrium constant; k: Rate constant; A: Frequency factor (L mol^{-1} s^{-1}); Ea: Activation energy of the reaction (kJ mol^{-1}); R: Universal gas constant (8.314 J mol^{-1} K^{-1}); T: Absolute temperature (K); X: Fraction of cemented antimony

Supplementary Information The online version contains supplementary material available at https://doi.org/10.1007/s42461-021-00489-6.

Acknowledgments This study is a part of the doctorate thesis of Mr. Özgün Küçükoğlu and was financially supported by the Marmara University Scientific Research Unit under the project FEN-C-DRP-090517-0283. The authors would like to thank American Manuscript Editors for editing the manuscript.

Author Contributions Serdar Aktas and Mehmet Hakan Morcali conceived and designed the study, and Özgün Küçükoğlu, performed the experiments. Özgün Küçükoğlu and Burcu Nilgun Cetiner wrote the manuscript. Serdar Aktas and Mehmet Hakan Morcali reviewed and edited the manuscript. All authors read and approved the manuscript.

Declarations

Conflict of Interest The authors declare that they have no conflict of interest.

References

1. Zhang Y, Kang S, Chen P, Li X, Liu Y, Gao T, Guo J, Sillanpää M (2016) Records of anthropogenic antimony in the glacial snow from the southeastern Tibetan plateau. J Asian Earth Sci 131:62–71
2. Léonard A, Gerber GB (1996) Mutagenicity, carcinogenicity and teratogenicity of antimony compounds. Mutat Res 366:1–8
3. Wilson NJ, Craw D, Hunter K (2004) Antimony distribution and environmental mobility at an historic antimony smelter site, New Zealand. Environ Pollut 129:257–266
4. Wilson SC, Lockwood PV, Ashley PM, Tighe M (2010) The chemistry and behaviour of antimony in the soil environment with comparisons to arsenic: a critical review. Environ Pollut 158:1169–1181
5. Okkenhaug G, Zhu Y-G, Luo L, Lei M, Li X, Jan Mulder J (2011) Distribution, speciation and availability of antimony (Sb) in soils and terrestrial plants from an active Sb mining area. Environ Pollut 159:2427–2434
6. Filella M, Belzile N, Chen YW (2002) Antimony in the environment: a review focused on natural waters I. Occurence. Earth-Science Rev 57:125–176. https://doi.org/10.1016/S0012-8252(01)00070-8
7. Abdul Nishad P, Bhaskarapillai A (2021) Antimony, a pollutant of emerging concern: a review on industrial sources and remediation technologies. Chemosphere 277:130252. https://doi.org/10.1016/j.chemosphere.2021.130252
8. Filella M, Belzile N, Chen YW (2002) Antimony in the environment: a review focused on natural waters II. Relevant solution chemistry. Earth-Science Rev 59:265–285. https://doi.org/10.1016/S0012-8252(02)00089-2
9. Herath I, Vithanage M, Bundschuh J (2017) Antimony as a global dilemma: geochemistry, mobility, fate and transport. Environ Pollut 223:545–559. https://doi.org/10.1016/j.envpol.2017.01.057
10. Cai Y, Mic Y, Zhang H (2016) Kinetic modeling of antimony(III) oxidation and sorption in soils. J Hazard Mater 316:102–109
11. Hiller E, Lalinská B, Chovan M, Jurkovicˇ L, Klimko T, Jankulár M, Hovorič R, Šottník P, Fľaková R, Ženišová Z, Ondrejková I (2012) Arsenic and antimony contamination of waters, stream sediments and soils in the vicinity of abandoned antimony mines in the Western Carpathians, Slovakia. Appl Geochem 27:598–614
12. Fernández MA, Segarra M, Espiell F (1996) Selective leaching of arsenic and antimony contained in the anode slimes from copper refining. Hydrometallurgy 41:255–267
13. Celep O, Alp İ, Deveci H (2011) Improved gold and silver extraction from a refractory antimony ore by pretreatment with alkaline sulphide leach. Hydrometallurgy 105:234–239
14. Yang T, Rao S, Liu W, Zhang D, Chen L (2017) A selective process for extracting antimony from refractory gold ore. Hydrometallurgy 169:571–575
15. Wikedzi A, Sandström Å, Awe SA (2016) Recovery of antimony compounds from alkaline sulphide leachates. Int J Miner Process 152:26–35
16. Ubaldini S, Vegliò F, Fornari P, Abbruzzese C (2000) Process flow-sheet for gold and antimony recovery from stibnite. Hydrometallurgy 57:187–199
17. Liu W, Yang T, Zhou Q, Zhang D, Lei C (2012) Electrodeposition of Sb(ċ) in alkaline solutions containing xylitol. Trans Nonferrous Met Soc China 22:949–957
18. Duchao Z, Tianzu Y, Wei L, Weifeng L, Zhaofeng X (2009) Electrorefining of a gold-bearing antimony alloy in alkaline xylitol solution. Hydrometallurgy 99:151–156
19. Awe SA, Sandström Å (2013) Electrowinning of antimony from model sulphide alkaline solutions. Hydrometallurgy 137:60–67
20. Awe SA, Sundkvist JE, Bolin NJ, Sandström Å (2013) Process flowsheet development for recovering antimony from Sb-bearing copper concentrates. Miner Eng 49:45–53
21. Zhu J, Wu F, Pan X, Guo J, Wen D (2011) Removal of antimony from antimony mine flotation wastewater by electrocoagulation with aluminum electrodes. J Environ Sci 23:1066–1071
22. Mahlangu T, Gudyanga FP, Simbi DJ (2006) Reductive leaching of stibnite (Sb_2S_3) flotation concentrate using metallic iron in a hydrochloric acid medium I: thermodynamics. Hydrometallurgy 84:192–203
23. Tian Q, Wang H, Xin Y, Li D, Guo X (2016) Ozonation leaching of a complex sulfidic antimony ore in hydrochloric acid solution. Hydrometallurgy 159:126–131

24. Guo X, Xin Y, Wang H, Tian Q (2017) Mineralogical characterization and pretreatment for antimony extraction by ozone of antimony-bearing refractory gold concentrates. Trans Nonferrous Met Soc China 27:1888–1895
25. Guo X, Xin Y, Wang H, Tian Q (2017) Leaching kinetics of antimony-bearing complex sulfides ore in hydrochloric acid solution with ozone. Trans Nonferrous Met Soc China 27:2073–2081
26. Yang J, Wu Y (2014) A hydrometallurgical process for the separation and recovery of antimony. Hydrometallurgy 143:68–74
27. Gu F, Summers PA, Hall P (2019) Recovering materials from waste mobile phones: recent technological developments. J Clean Prod 237:117657
28. Aktas S (2011) Rhodium recovery from rhodium-containing waste rinsing water via cementation using zinc powder. Hydrometallurgy 106:71–75
29. Farahmand F, Moradkhani D, Safarzadeh MS, Rashchi F (2009) Optimization and kinetics of the cementation of lead with aluminum powder. Hydrometallurgy 98:81–85
30. Aktas S (2010) Silver recovery from spent silver oxide button cells. Hydrometallurgy 104:106–111
31. Nosier SA, Sallam SA (2000) Removal of lead ions from wastewater by cementation on a gas-sparged zinc cylinder. Sep Purif Technol 18:93–101
32. Dib A, Makhloufi L (2004) Cementation treatment of copper in wastewater: mass transfer in a fixed bed of iron spheres. Chem Eng Process 43:1265–1273
33. Fouad OA, Abdel SM (2005) Cementation-induced recovery of self-assembled ultrafine copper powders from spent etching solutions of printed circuit board. Powder Technol 159:127–134
34. Power GP, Ritchie IM (1976) A contribution to the theory of cementation (metal displacement) reactions. Aust J Chem 29:699–709
35. Demirkiran N, Ekmekyapar A, Künkül A, Baysar A (2007) A kinetic study of copper cementation with zinc in aqueous solutions. Int J Miner Process 82:80–85
36. Noubactep C (2010) Elemental metals for environmental remediation: learning from cementation process. J Hazard Mater 181:1170–1174
37. https://opentextbc.ca/introductorychemistry/back-matter/appendix-standard-reduction-potentials-by-value-2 /. Accessed 20 Sept 2020
38. Van der Pas V, Dreisinger D (1996) A fundamental study of cobalt cementation by zinc dust in the presence of copper and antimony additives. Hydrometallurgy 43:187–205
39. Shamsuddin M (2016) Physical chemistry of metallurgical processes. Wiley, Hoboken
40. Aktaş S, Çetiner BN (2020) Investigation of alkaline leaching parameters on stibnite concentrate. Mining, Metallurgy & Exploration 37:1729–1739
41. https://www.lme.com/ Accessed 12 Aug 2021
42. https://www.usantimony.com/antimony-prices/ Accessed 12 Aug 2021